Chapter 4

Equations Governing Geophysical Flows

ABSTRACT

This chapter continues the development of the equations that form the basis of dynamical meteorology and physical oceanography. Averaging is performed over turbulent fluctuations and further simplifications are justified based on a scale analysis. In the process, some important dimensionless numbers are introduced. The need for an appropriate set of initial and boundary conditions is also explored from mathematical, physical, and numerical points of view.

4.1 REYNOLDS-AVERAGED EQUATIONS

Geophysical flows are typically in a state of turbulence, and most often we are only interested in the statistically averaged flow, leaving aside all turbulent fluctuations. To this effect and following Reynolds (1894), we decompose each variable into a mean, denoted with a set of brackets, and a fluctuation, denoted by a prime:

$$u = \langle u \rangle + u', \tag{4.1}$$

such that $\langle u' \rangle = 0$ by definition.

There are several ways to define the averaging process, some more rigorous than others, but we shall not be concerned here with those issues, preferring to think of the mean as a temporal average over rapid turbulent fluctuations, on a time interval long enough to obtain a statistically significant mean, yet short enough to retain the slower evolution of the flow under consideration. Our hypothesis is that such an intermediate time interval exists.

Quadratic expressions such as the product uv of two velocity components have the following property:

$$\begin{aligned} \langle uv \rangle &= \langle \langle u \rangle \langle v \rangle \rangle + \cancelto{=0}{\langle \langle u \rangle v' \rangle} + \cancelto{=0}{\langle \langle v \rangle u' \rangle} + \langle u'v' \rangle \\ &= \langle u \rangle \langle v \rangle + \langle u'v' \rangle \end{aligned} \tag{4.2}$$

Introduction to Geophysical Fluid Dynamics, Volume 101, ISSN 0074-6142, DOI: 10.1016/B978-0-12-088759-0.00004-3

and similarly for $\langle uu\rangle$, $\langle uw\rangle$, $\langle u\rho\rangle$, etc. We recognize here that the average of a product is not equal to the product of the averages. This is a double-edged sword: On one hand, it generates mathematical complications but on the other hand, it also creates interesting situations.

Our objective is to establish equations governing the mean quantities, $\langle u\rangle$, $\langle v\rangle$, $\langle w\rangle$, $\langle p\rangle$, and $\langle\rho\rangle$. Starting with the average of the x-momentum equation (3.19), we have

$$\frac{\partial\langle u\rangle}{\partial t}+\frac{\partial\langle uu\rangle}{\partial x}+\frac{\partial\langle vu\rangle}{\partial y}+\frac{\partial\langle wu\rangle}{\partial z}+f_*\langle w\rangle-f\langle v\rangle=-\frac{1}{\rho_0}\frac{\partial\langle p\rangle}{\partial x}+\nu\nabla^2\langle u\rangle, \quad (4.3)$$

which becomes

$$\begin{aligned}\frac{\partial\langle u\rangle}{\partial t}+\frac{\partial(\langle u\rangle\langle u\rangle)}{\partial x}+\frac{\partial(\langle u\rangle\langle v\rangle)}{\partial y}+\frac{\partial(\langle u\rangle\langle w\rangle)}{\partial z}+f_*\langle w\rangle-f\langle v\rangle\\ =-\frac{1}{\rho_0}\frac{\partial\langle p\rangle}{\partial x}+\nu\nabla^2\langle u\rangle-\frac{\partial\langle u'u'\rangle}{\partial x}-\frac{\partial\langle u'v'\rangle}{\partial y}-\frac{\partial\langle u'w'\rangle}{\partial z}. \quad (4.4)\end{aligned}$$

We note that this last equation for the mean velocity looks identical to the original equation, except for the presence of three new terms at the end of the right-hand side. These terms represent the effects of the turbulent fluctuations on the mean flow. Combining these terms with corresponding frictional terms

$$\frac{\partial}{\partial x}\left(\nu\frac{\partial\langle u\rangle}{\partial x}-\langle u'u'\rangle\right),\quad \frac{\partial}{\partial y}\left(\nu\frac{\partial\langle u\rangle}{\partial y}-\langle u'v'\rangle\right),\quad \frac{\partial}{\partial z}\left(\nu\frac{\partial\langle u\rangle}{\partial z}-\langle u'w'\rangle\right)$$

indicates that the averages of velocity fluctuations add to the viscous stresses (e.g., $-\langle u'w'\rangle$ adds to $\nu\partial\langle u\rangle/\partial z$) and can therefore be considered frictional stresses caused by turbulence. To give credit to Osborne Reynolds who first decomposed the flow into mean and fluctuating components, the expressions $-\langle u'u'\rangle$, $-\langle u'v'\rangle$, and $-\langle u'w'\rangle$ are called *Reynolds stresses*. Since they do not have the same form as the viscous stresses, it can be said that the mean turbulent flow behaves as a fluid governed by a frictional law other than that of viscosity. In other words, a turbulent flow behaves as a non-Newtonian fluid.

Similar averages of the y- and z-momentum equations (3.20)–(3.22) over the turbulent fluctuations yield

$$\begin{aligned}\frac{\partial\langle v\rangle}{\partial t}+\frac{\partial(\langle u\rangle\langle v\rangle)}{\partial x}+\frac{\partial(\langle v\rangle\langle v\rangle)}{\partial y}+\frac{\partial(\langle v\rangle\langle w\rangle)}{\partial z}+f\langle u\rangle+\frac{1}{\rho_0}\frac{\partial\langle p\rangle}{\partial y}\\ =\frac{\partial}{\partial x}\left(\nu\frac{\partial\langle v\rangle}{\partial x}-\langle u'v'\rangle\right)+\frac{\partial}{\partial y}\left(\nu\frac{\partial\langle v\rangle}{\partial y}-\langle v'v'\rangle\right)+\frac{\partial}{\partial z}\left(\nu\frac{\partial\langle v\rangle}{\partial z}-\langle v'w'\rangle\right)\end{aligned} \quad (4.5)$$

$$\frac{\partial\langle w\rangle}{\partial t}+\frac{\partial(\langle u\rangle\langle w\rangle)}{\partial x}+\frac{\partial(\langle v\rangle\langle w\rangle)}{\partial y}+\frac{\partial(\langle w\rangle\langle w\rangle)}{\partial z}-f_*\langle u\rangle+\frac{1}{\rho_0}\frac{\partial\langle p\rangle}{\partial z}=-g\langle\rho\rangle$$
$$+\frac{\partial}{\partial x}\left(\nu\frac{\partial\langle w\rangle}{\partial x}-\langle u'w'\rangle\right)+\frac{\partial}{\partial y}\left(\nu\frac{\partial\langle w\rangle}{\partial y}-\langle v'w'\rangle\right)+\frac{\partial}{\partial z}\left(\nu\frac{\partial\langle w\rangle}{\partial z}-\langle w'w'\rangle\right). \tag{4.6}$$

4.2 EDDY COEFFICIENTS

Computer models of geophysical fluid systems are limited in their spatial resolution. They are therefore incapable of resolving all but the largest turbulent fluctuations, and all motions of lengths shorter than the mesh size. In one way or another, we must state something about these unresolved turbulent and subgrid scale motions in order to incorporate their aggregate effect on the larger, resolved flow. This process is called *subgrid-scale parameterization*. Here, we present the simplest of all schemes. More sophisticated parameterizations will follow in later sections of the book, particularly Chapter 14.

The primary effect of fluid turbulence and of motions at subgrid scales (small eddies and billows) is dissipation. It is therefore tempting to represent both the Reynolds stress and the effect of unresolved motions as some form of super viscosity. This is done summarily by replacing the molecular viscosity ν of the fluid by a much larger *eddy viscosity* to be defined in terms of turbulence and grid properties. This rather crude approach was first proposed by Boussinesq.

However, the parameterization recognizes one essential property: the anisotropy of the flow field and its modeling grid. Horizontal and vertical directions are treated differently by assigning two distinct eddy viscosities, $\mathcal{A}$ in the horizontal and ν_E in the vertical. Because turbulent motions and mesh size cover longer distances in the horizontal than in the vertical, $\mathcal{A}$ covers a much larger span of unresolved motions and needs to be significantly larger than ν_E. Furthermore, as they ought to depend in some elementary way on flow properties and grid dimensions, each of which may vary from place to place, eddy viscosities should be expected to exhibit some spatial variations. Returning to the basic manner by which the momentum budget was established, with stress differentials among forces on the right-hand sides, we are led to retain these eddy coefficients inside the first derivatives as follows:

$$\frac{\partial u}{\partial t}+u\frac{\partial u}{\partial x}+v\frac{\partial u}{\partial y}+w\frac{\partial u}{\partial z}+f_*w-fv$$
$$=-\frac{1}{\rho_0}\frac{\partial p}{\partial x}+\frac{\partial}{\partial x}\left(\mathcal{A}\frac{\partial u}{\partial x}\right)+\frac{\partial}{\partial y}\left(\mathcal{A}\frac{\partial u}{\partial y}\right)+\frac{\partial}{\partial z}\left(\nu_E\frac{\partial u}{\partial z}\right), \tag{4.7a}$$

$$\frac{\partial v}{\partial t}+u\frac{\partial v}{\partial x}+v\frac{\partial v}{\partial y}+w\frac{\partial v}{\partial z}+fu$$
$$=-\frac{1}{\rho_0}\frac{\partial p}{\partial y}+\frac{\partial}{\partial x}\left(\mathcal{A}\frac{\partial v}{\partial x}\right)+\frac{\partial}{\partial y}\left(\mathcal{A}\frac{\partial v}{\partial y}\right)+\frac{\partial}{\partial z}\left(\nu_E\frac{\partial v}{\partial z}\right), \tag{4.7b}$$

$$\frac{\partial w}{\partial t}+u\frac{\partial w}{\partial x}+v\frac{\partial w}{\partial y}+w\frac{\partial w}{\partial z}-f_*u$$
$$=-\frac{1}{\rho_0}\frac{\partial p}{\partial z}-\frac{g\rho}{\rho_0}+\frac{\partial}{\partial x}\left(\mathcal{A}\frac{\partial w}{\partial x}\right)+\frac{\partial}{\partial y}\left(\mathcal{A}\frac{\partial w}{\partial y}\right)+\frac{\partial}{\partial z}\left(\nu_{\mathrm{E}}\frac{\partial w}{\partial z}\right), \quad (4.7c)$$

Since we will work exclusively with averaged equations in the rest of the book (unless otherwise specified), there is no longer any need to denote averaged quantities with brackets. Consequently, $\langle u\rangle$ has been replaced by u and similarly for all other variables.

In the energy (density) equation, heat and salt molecular diffusion needs likewise to be superseded by the dispersing effect of unresolved turbulent motions and subgrid-scale processes. Using the same horizontal eddy viscosity $\mathcal{A}$ for energy as for momentum is generally adequate, because the larger turbulent motions and subgrid processes act to disperse heat and salt as effectively as momentum. However, in the vertical, the practice is usually to distinguish dispersion of energy from that of momentum by introducing a vertical *eddy diffusivity* κ_{E} that differs from the vertical eddy viscosity ν_{E}. This difference stems from the specific turbulent behavior of each state variable and will be further discussed in Section 14.3. The energy (density) equation then becomes

$$\frac{\partial \rho}{\partial t}+u\frac{\partial \rho}{\partial x}+v\frac{\partial \rho}{\partial y}+w\frac{\partial \rho}{\partial z}$$
$$=\frac{\partial}{\partial x}\left(\mathcal{A}\frac{\partial \rho}{\partial x}\right)+\frac{\partial}{\partial y}\left(\mathcal{A}\frac{\partial \rho}{\partial y}\right)+\frac{\partial}{\partial z}\left(\kappa_{\mathrm{E}}\frac{\partial \rho}{\partial z}\right). \quad (4.8)$$

The linear continuity equation is not subjected to any such adaptation and remains unchanged:

$$\frac{\partial u}{\partial x}+\frac{\partial v}{\partial y}+\frac{\partial w}{\partial z}=0. \quad (4.9)$$

For more details on eddy viscosity and diffusivity and some schemes to make those depend on flow properties, the reader is referred to textbooks on turbulence, such as Tennekes and Lumley (1972) or Pope (2000). A widely used method to incorporate subgrid-scale processes in the horizontal eddy viscosity is that proposed by Smagorinsky (1963):

$$\mathcal{A}=\Delta x\Delta y\sqrt{\left(\frac{\partial u}{\partial x}\right)^2+\left(\frac{\partial v}{\partial y}\right)^2+\frac{1}{2}\left(\frac{\partial u}{\partial y}+\frac{\partial v}{\partial x}\right)^2}, \quad (4.10)$$

in which Δx and Δy are the local grid dimensions. Because the horizontal eddy viscosity is meant to represent physical processes, it ought to obey certain symmetry properties, notably invariance with respect to rotation of the coordinate system in the horizontal plane. We leave it to the reader to verify that the preceding formulation for $\mathcal{A}$ does indeed meet this requirement.

4.3 SCALES OF MOTION

Simplifications of the equations established in the preceding section are possible beyond the Boussinesq approximation and averaging over turbulent fluctuations. However, these require a preliminary discussion of orders of magnitude. Accordingly, let us introduce a scale for every variable, as we already did in a limited way in Section 1.10. By *scale*, we mean a dimensional constant of dimensions identical to that of the variable and having a numerical value representative of the values of that same variable. Table 4.1 provides illustrative scales for the variables of interest in geophysical fluid flow. Obviously, scale values do vary with every application, and the values listed in Table 4.1 are only suggestive. Even so, the conclusions drawn from the use of these particular values stand in the vast majority of cases. If doubt arises in a specific situation, the following scale analysis can always be redone.

In the construction of Table 4.1, we were careful to satisfy the criteria of geophysical fluid dynamics outlined in Sections 1.5 and 1.6,

$$T \gtrsim \frac{1}{\Omega}, \tag{4.11}$$

for the time scale and

$$\frac{U}{L} \lesssim \Omega, \tag{4.12}$$

for the velocity and length scales. It is generally not required to discriminate between the two horizontal directions, and we assign the same length scale L to both coordinates and the same velocity scale U to both velocity components. However, the same cannot be said of the vertical direction. Geophysical flows are typically confined to domains that are much wider than they are thick, and the *aspect ratio* H/L is small. The atmospheric layer that determines our weather is only about 10 km thick, yet cyclones and anticyclones spread over thousands of kilometers. Similarly, ocean currents are generally confined to the upper hundred meters of the water column but extend over tens of kilometers or more, up

TABLE 4.1 Typical Scales of Atmospheric and Oceanic Flows

Variable	Scale	Unit	Atmospheric Value	Oceanic Value
x, y	L	m	$100\ \text{km} = 10^5\ \text{m}$	$10\ \text{km} = 10^4\ \text{m}$
z	H	m	$1\ \text{km} = 10^3\ \text{m}$	$100\ \text{m} = 10^2\ \text{m}$
t	T	s	$\geq \frac{1}{2}\ \text{day} \simeq 4 \times 10^4\ \text{s}$	$\geq 1\ \text{day} \simeq 9 \times 10^4\ \text{s}$
u, v	U	m/s	10 m/s	0.1 m/s
w	W	m/s		
p	P	$\text{kg m}^{-1}\,\text{s}^{-2}$	variable	
ρ	$\Delta\rho$	kg/m^3		

to the width of the ocean basin. It follows that for large-scale motions,

$$H \ll L, \tag{4.13}$$

and we expect W to be vastly different from U.

The continuity equation in its reduced form (4.9) contains three terms of respective orders of magnitude:

$$\frac{U}{L}, \quad \frac{U}{L}, \quad \frac{W}{H}.$$

We ought to examine three cases: W/H is much less than, on the order of, or much greater than U/L. The third case must be ruled out. Indeed, if $W/H \gg U/L$, the equation reduces in first approximation to $\partial w/\partial z = 0$, which implies that w is constant in the vertical; because of a bottom somewhere, that flow must be supplied by lateral convergence (see later section 4.6.1), and we deduce that the terms $\partial u/\partial x$ and/or $\partial v/\partial y$ may not be both neglected at the same time. In sum, w must be much smaller than initially thought.

In the first case, the leading balance is two dimensional, $\partial u/\partial x + \partial v/\partial y = 0$, which implies that convergence in one horizontal direction must be compensated by divergence in the other horizontal direction. This is very possible. The intermediate case, with W/H on the order of U/L, implies a three-way balance, which is also acceptable. In summary, the vertical-velocity scale must be constrained by

$$W \lesssim \frac{H}{L} U \tag{4.14}$$

and, by virtue of Eq. (4.13),

$$W \ll U. \tag{4.15}$$

In other words, large-scale geophysical flows are shallow ($H \ll L$) and nearly two-dimensional ($W \ll U$).

Let us now consider the x-momentum equation in its Boussinesq and turbulence-averaged form (4.7a). Its various terms scale sequentially as

$$\frac{U}{T}, \quad \frac{U^2}{L}, \quad \frac{U^2}{L}, \quad \frac{WU}{H}, \quad \Omega W, \quad \Omega U, \quad \frac{P}{\rho_0 L}, \quad \frac{\mathcal{A}U}{L^2}, \quad \frac{\mathcal{A}U}{L^2}, \quad \frac{\nu_E U}{H^2}.$$

The previous remark immediately shows that the fifth term (ΩW) is always much smaller than the sixth (ΩU) and can be safely neglected.[1]

[1] Note, however, that near the equator, where f goes to zero while f_* reaches its maximum, the simplification may be invalidated. If this is the case, a reexamination of the scales is warranted. The fifth term is likely to remain much smaller than some other terms, such as the pressure gradient, but there may be instances when the f_* term must be retained. Because such a situation is exceptional, we will dispense with the f_* term here.

Because of the fundamental importance of the rotation terms in geophysical fluid dynamics, we can anticipate that the pressure-gradient term (the driving force) will scale as the Coriolis terms, that is,

$$\frac{P}{\rho_0 L} = \Omega U \quad \rightarrow \quad P = \rho_0 \Omega L U. \tag{4.16}$$

For typical geophysical flows, this dynamic pressure is much smaller than the basic hydrostatic pressure due to the weight of the fluid.

Although horizontal and vertical dissipations due to turbulent and subgrid-scale processes is retained in the equation (its last three terms), it cannot dominate the Coriolis force in geophysical flows, which ought to remain among the dominant terms. This implies

$$\frac{\mathcal{A}U}{L^2} \quad \text{and} \quad \frac{\nu_E U}{H^2} \lesssim \Omega U. \tag{4.17}$$

Similar considerations apply to the y-momentum equation (4.7b). But the vertical momentum equation (4.7c) may be subjected to additional simplifications. Its various terms scale sequentially as

$$\frac{W}{T}, \quad \frac{UW}{L}, \quad \frac{UW}{L}, \quad \frac{W^2}{H}, \quad \Omega U, \quad \frac{P}{\rho_0 H}, \quad \frac{g\Delta\rho}{\rho_0}, \quad \frac{\mathcal{A}W}{L^2}, \quad \frac{\mathcal{A}W}{L^2}, \quad \frac{\nu_E W}{H^2}.$$

The first term (W/T) cannot exceed ΩW, which is itself much less than ΩU, by virtue of Eqs. (4.11) and (4.15). The next three terms are also much smaller than ΩU; this time because of Eqs. (4.12), (4.14), and (4.15). Thus, the first four terms may all be neglected compared to the fifth. But this fifth term is itself quite small. Its ratio to the first term on the right-hand side is

$$\frac{\rho_0 \Omega H U}{P} \sim \frac{H}{L},$$

which according to Eqs. (4.16) and (4.13) is much less than 1.

Finally, the last three terms are small. When W is substituted for U in Eq. (4.17), we have

$$\frac{\mathcal{A}W}{L^2} \quad \text{and} \quad \frac{\nu_E W}{H^2} \lesssim \Omega W \ll \Omega U. \tag{4.18}$$

Thus, the last three terms on the right-hand side of the equation are much less than the fifth term on the left, which was already found to be very small. In summary, only two terms remain, and the vertical-momentum balance reduces to the simple *hydrostatic balance*:

$$0 = -\frac{1}{\rho_0}\frac{\partial p}{\partial z} - \frac{g\rho}{\rho_0}. \tag{4.19}$$

In the absence of stratification (density perturbation ρ nil), the next term in line that should be considered a possible balance to the pressure gradient

$(1/\rho_0)(\partial p/\partial z)$ is $f_* u$. However, under such balance, the vertical variation of the pressure p would be given by the vertical integration of $\rho_0 f_* u$ and its scale be $\rho_0 \Omega H U$. Since this is much less than the already established pressure scale (4.16), it is negligible, and we conclude that the vertical variation of p is very weak. In other words, p is nearly z-independent in the absence of stratification:

$$0 = -\frac{1}{\rho_0}\frac{\partial p}{\partial z}. \tag{4.20}$$

So, the hydrostatic balance (4.19) continues to hold in the limit $\rho \to 0$.

Since the pressure p is already a small perturbation to a much larger pressure, itself in hydrostatic balance, we conclude that geophysical flows tend to be fully hydrostatic even in the presence of substantial motions.[2] Looking back, we note that the main reason behind this reduction is the strong geometric disparity of geophysical flows ($H \ll L$).

In rare instances when this disparity between horizontal and vertical scales does not exist, such as in convection plumes and short internal waves, the hydrostatic approximation ceases to hold and the vertical-momentum balance includes a three-way balance between vertical acceleration, pressure gradient, and buoyancy.

4.4 RECAPITULATION OF EQUATIONS GOVERNING GEOPHYSICAL FLOWS

The Boussinesq approximation performed in the previous chapter and the preceding developments have greatly simplified the equations. We recapitulate them here.

$$\begin{aligned} x\text{-momentum: } & \frac{\partial u}{\partial t} + u\frac{\partial u}{\partial x} + v\frac{\partial u}{\partial y} + w\frac{\partial u}{\partial z} - fv \\ & = -\frac{1}{\rho_0}\frac{\partial p}{\partial x} + \frac{\partial}{\partial x}\left(\mathcal{A}\frac{\partial u}{\partial x}\right) + \frac{\partial}{\partial y}\left(\mathcal{A}\frac{\partial u}{\partial y}\right) + \frac{\partial}{\partial z}\left(\nu_{\mathrm{E}}\frac{\partial u}{\partial z}\right) \end{aligned} \tag{4.21a}$$

$$\begin{aligned} y\text{-momentum: } & \frac{\partial v}{\partial t} + u\frac{\partial v}{\partial x} + v\frac{\partial v}{\partial y} + w\frac{\partial v}{\partial z} + fu \\ & = -\frac{1}{\rho_0}\frac{\partial p}{\partial y} + \frac{\partial}{\partial x}\left(\mathcal{A}\frac{\partial v}{\partial x}\right) + \frac{\partial}{\partial y}\left(\mathcal{A}\frac{\partial v}{\partial y}\right) + \frac{\partial}{\partial z}\left(\nu_{\mathrm{E}}\frac{\partial v}{\partial z}\right) \end{aligned} \tag{4.21b}$$

[2] According to Nebeker (1995, page 51), the scientist deserving credit for the hydrostatic balance in geophysical flows is Alexis Clairaut (1713–1765).

$$z\text{-momentum: } 0 = -\frac{\partial p}{\partial z} - \rho g \tag{4.21c}$$

$$\text{continuity: } \frac{\partial u}{\partial x} + \frac{\partial v}{\partial y} + \frac{\partial w}{\partial z} = 0 \tag{4.21d}$$

$$\text{energy: } \frac{\partial \rho}{\partial t} + u\frac{\partial \rho}{\partial x} + v\frac{\partial \rho}{\partial y} + w\frac{\partial \rho}{\partial z} = \frac{\partial}{\partial x}\left(\mathcal{A}\frac{\partial \rho}{\partial x}\right) + \frac{\partial}{\partial y}\left(\mathcal{A}\frac{\partial \rho}{\partial y}\right) + \frac{\partial}{\partial z}\left(\kappa_E\frac{\partial \rho}{\partial z}\right), \tag{4.21e}$$

where the reference density ρ_0 and the gravitational acceleration g are constant coefficients, the Coriolis parameter $f = 2\Omega\sin\varphi$ is dependent on latitude or taken as a constant, and the eddy viscosity and diffusivity coefficients $\mathcal{A}$, ν_E, and κ_E may be taken as constants or functions of flow variables and grid parameters. These five equations for the five variables u, v, w, p, and ρ form a closed set of equations, the cornerstone of geophysical fluid dynamics, sometimes called *primitive equations*.

Using the continuity equation (4.21d), the horizontal-momentum and density equations can be written in *conservative form*:

$$\frac{\partial u}{\partial t} + \frac{\partial (uu)}{\partial x} + \frac{\partial (vu)}{\partial y} + \frac{\partial (wu)}{\partial z} - fv = -\frac{1}{\rho_0}\frac{\partial p}{\partial x} + \frac{\partial}{\partial x}\left(\mathcal{A}\frac{\partial u}{\partial x}\right) + \frac{\partial}{\partial y}\left(\mathcal{A}\frac{\partial u}{\partial y}\right) + \frac{\partial}{\partial z}\left(\nu_E\frac{\partial u}{\partial z}\right) \tag{4.22a}$$

$$\frac{\partial v}{\partial t} + \frac{\partial (uv)}{\partial x} + \frac{\partial (vv)}{\partial y} + \frac{\partial (wv)}{\partial z} + fu = -\frac{1}{\rho_0}\frac{\partial p}{\partial y} + \frac{\partial}{\partial x}\left(\mathcal{A}\frac{\partial v}{\partial x}\right) + \frac{\partial}{\partial y}\left(\mathcal{A}\frac{\partial v}{\partial y}\right) + \frac{\partial}{\partial z}\left(\nu_E\frac{\partial v}{\partial z}\right) \tag{4.22b}$$

$$\frac{\partial \rho}{\partial t} + \frac{\partial (u\rho)}{\partial x} + \frac{\partial (v\rho)}{\partial y} + \frac{\partial (w\rho)}{\partial z} = \frac{\partial}{\partial x}\left(\mathcal{A}\frac{\partial \rho}{\partial x}\right) + \frac{\partial}{\partial y}\left(\mathcal{A}\frac{\partial \rho}{\partial y}\right) + \frac{\partial}{\partial z}\left(\kappa_E\frac{\partial \rho}{\partial z}\right), \tag{4.22c}$$

These will be found useful in numerical discretization.

4.5 IMPORTANT DIMENSIONLESS NUMBERS

The scaling analysis of Section 4.3 was developed to justify the neglect of some small terms. But this does not necessarily imply that the remaining terms are equally large. We now wish to estimate the relative sizes of those terms that have been retained.

The terms of the horizontal momentum equations in their last form (4.21a) and (4.21b) scale sequentially as

$$\frac{U}{T}, \quad \frac{U^2}{L}, \quad \frac{U^2}{L}, \quad \frac{WU}{H}, \quad \Omega U, \quad \frac{P}{\rho_0 L}, \quad \frac{\mathcal{A}U}{L^2}, \quad \frac{\nu_E U}{H^2}.$$

By definition, geophysical fluid dynamics treats those motions in which rotation is an important factor. Thus, the term ΩU is central to the preceding sequence. A division by ΩU, to measure the importance of all other terms relative to the Coriolis term, yields the following sequence of dimensionless ratios:

$$\frac{1}{\Omega T}, \quad \frac{U}{\Omega L}, \quad \frac{U}{\Omega L}, \quad \frac{WL}{UH}\cdot\frac{U}{\Omega L}, \quad 1, \quad \frac{P}{\rho_0 \Omega L U}, \quad \frac{\mathcal{A}}{\Omega L^2}, \quad \frac{\nu_E}{\Omega H^2}.$$

The first ratio,

$$Ro_T = \frac{1}{\Omega T}, \tag{4.23}$$

is called the *temporal Rossby number*. It compares the local time rate of change of the velocity to the Coriolis force and is on the order of unity or less as has been repeatedly stated, see Eq. (4.11). The next number,

$$Ro = \frac{U}{\Omega L}, \tag{4.24}$$

which compares advection to Coriolis force, is called the *Rossby number*[3] and is fundamental in geophysical fluid dynamics. Like its temporal analogue Ro_T, it is at most on the order of unity by virtue of Eq. (4.12). As a general rule, the characteristics of geophysical flows vary greatly with the values of the Rossby numbers.

The next number is the product of the Rossby number by WL/UH, which is on the order of 1 or less by virtue of Eq. (4.14). It will be shown in Section 11.5 that the ratio WL/UH is generally on the order of the Rossby number itself. The next ratio, $P/\rho_0 \Omega L U$, is on the order of unity by virtue of Eq. (4.16).

The last two ratios measure the relative importance of horizontal and vertical frictions. Of the two, only the latter bears a name:

$$Ek = \frac{\nu_E}{\Omega H^2}, \tag{4.25}$$

is called the *Ekman number*. For geophysical flows, this number is small. For example, with an eddy viscosity ν_E as large as $10^{-2}\text{m}^2/\text{s}$, $\Omega = 7.3 \times 10^{-5}\ \text{s}^{-1}$ and $H = 100$ m, $Ek = 1.4 \times 10^{-2}$. The Ekman number is even smaller in laboratory experiments where the viscosity reverts to its molecular value and the height scale H is much more modest. [Typical experimental values are

[3] See biographic note at the end of this chapter.

$\Omega = 4\ \mathrm{s}^{-1}$, $H = 20\,\mathrm{cm}$, and $\nu(\text{water}) = 10^{-6}\,\mathrm{m}^2/\mathrm{s}$, yielding $Ek = 6 \times 10^{-6}$.] Although the Ekman number is small, indicating that the dissipative terms in the momentum equation may be negligible, these need to be retained. The reason will become clear in Chapter 8, when it is shown that vertical friction creates a very important boundary layer.

In nonrotating fluid dynamics, it is customary to compare inertial and frictional forces by defining the *Reynolds number*, *Re*. In the preceding scaling, inertial and frictional forces were not compared to each other, but each was instead compared to the Coriolis force, yielding the Rossby and Ekman numbers. There exists a simple relationship between the three numbers and the aspect ratio H/L:

$$Re = \frac{UL}{\nu_E} = \frac{U}{\Omega L} \cdot \frac{\Omega H^2}{\nu_E} \cdot \frac{L^2}{H^2} = \frac{Ro}{Ek}\left(\frac{L}{H}\right)^2. \tag{4.26}$$

Since the Rossby number is on the order of unity or slightly less, but the Ekman number and the aspect ratio H/L are both much smaller than unity, the Reynolds number of geophysical flows is extremely large, even after the molecular viscosity has been replaced by a much larger eddy viscosity.

With Eq. (4.16), the two terms in the hydrostatic equation (4.21c) scale, respectively, as

$$\frac{P}{H}, \quad g\Delta\rho$$

and the ratio of the latter over the former is

$$\frac{gH\Delta\rho}{P} = \frac{gH\Delta\rho}{\rho_0 \Omega L U} = \frac{U}{\Omega L} \cdot \frac{gH\Delta\rho}{\rho_0 U^2} = Ro \cdot \frac{gH\Delta\rho}{\rho_0 U^2}.$$

This leads to the additional dimensionless ratio

$$Ri = \frac{gH\Delta\rho}{\rho_0 U^2}, \tag{4.27}$$

which we already encountered in Section 1.6. It is called the *Richardson number*.[4] For geophysical flows, this number may be much less than, on the order of, or much greater than unity, depending on whether stratification effects are negligible, important, or dominant.

4.6 BOUNDARY CONDITIONS

The equations of Section 4.4 governing geophysical flows form a closed set of equations, with the number of unknown functions being equal to the number

[4] See biography at the end of Chapter 14

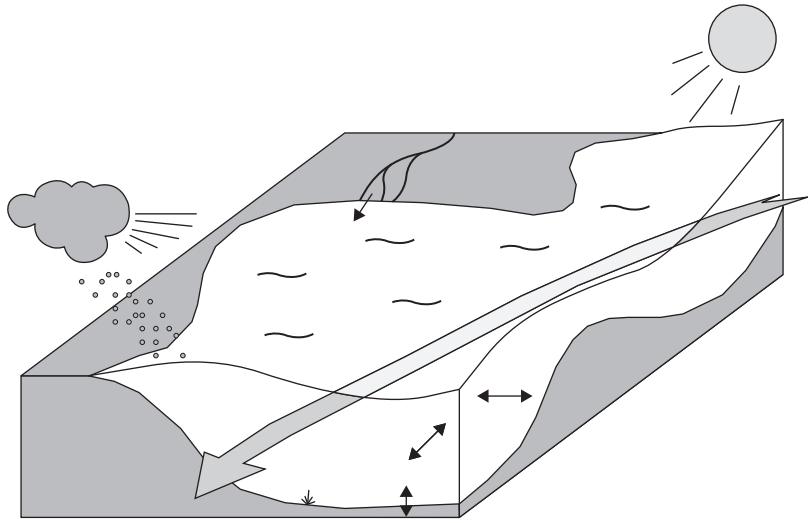

FIGURE 4.1 Schematic representation of possible exchanges between a coastal system under investigation and the surrounding environment. Boundary conditions must specify the influence of this outside world on the evolution within the domain. Exchanges may take place at the air–sea interface, in bottom layers, along coasts, and/or at any other boundary of the domain.

of available independent equations. However, the solution of those equations is uniquely defined only when additional specifications are provided. Those auxiliary conditions concern information on the initial state and geographical boundaries of the system (Fig. 4.1).

Because the governing equations (4.21) contain first-order time derivatives of u, v, and ρ, *initial conditions* are required, one for each of these three-dimensional fields. Because the respective equations, (4.21a), (4.21b), and (4.21e), provide *tendencies* for these variables in order to calculate future *values*, it is necessary to specify from where to start. The variables for which such initial conditions are required are called *state variables*. The remaining variables w and p, which have no time derivative in the equations, are called *diagnostic* variables, that is, they are variables that can be determined at any moment from the knowledge of the other variables at the same moment. Note that if a nonhydrostatic formalism is retained, the time derivative of the vertical velocity arises [see (4.7c)], and w passes from being a diagnostic variable to a state variable, and an initial condition becomes necessary for it, too.

The determination of pressure needs special care depending on whether the hydrostatic approximation is applied and on the manner in which sea surface height is modeled. Since the pressure gradient is a major force in geophysical flows, the handling of pressure is a central question in the development of GFD models. This point deserves a detailed analysis, which we postpone to Section 7.6.

The conditions to impose at *spatial* boundaries of the domain are more difficult to ascertain than initial conditions. The mathematical theory of partial differential equations teaches us that the number and type of required boundary conditions depend on the nature of the partial differential equations. Standard classification (e.g., Durran, 1999) of second-order partial differential equations makes the distinction between *hyperbolic*, *parabolic*, and *elliptic* equations. This classification is based on the concept of *characteristics*, which are lines along which information propagates. The geometry of these lines constrains where information is propagated from the boundary into the domain or from the domain outward across the boundary and therefore prescribes along which portion of the domain's boundary information needs to be specified in order to define uniquely the solution within the domain.

A major problem with the GFD governing equations is that their classification cannot be established once and for all. First, the coupled set of equations (4.21) is more complicated than a single second-order equation for which standard classification can be performed; second, the equation type can change with the solution itself. Indeed, propagation of information is mostly accomplished by a combination of flow advection and wave propagation, and these may at various times leave and enter through the same boundary segment. Thus, the number and type of required boundary conditions is susceptible to change over time with the solution of the problem, which is obviously not known a priori. It is far from a trivial task to establish the mathematically correct set of boundary conditions, and the reader is referred to specialized literature for further information (e.g., Blayo & Debreu, 2005; Durran, 1999). The imposition of boundary conditions during analytical studies in this book will be guided by purely physical arguments, and the well-behaved nature of the subsequent solution will serve as a posteriori verification.

For the many situations when no analytical solution is available, not only is a posteriori verification out of the question but the problem is further complicated by the fact that numerical discretization solves modified equations with truncation errors, rather than the original equations. The equations may demand fewer or more boundary and initial conditions. If the numerical scheme asks for more conditions than those provided by the original equations, these conditions must be related to the truncation error in such a way that they disappear when the grid size (or time step) vanishes: We demand that all boundary and initial conditions be consistent.

Let us, for example, revisit the initialization problem of the leapfrog scheme from this point of view. As we have seen (Section 2.9), the leapfrog discretization $\partial u/\partial t = Q \rightarrow \tilde{u}^{n+1} = \tilde{u}^{n-1} + 2\Delta t Q^n$ needs two values, $\tilde{u}^0$ and $\tilde{u}^1$, to start the time stepping. However, the original problem indicates that only one initial condition, $\tilde{u}^0$, may be imposed, the value of which is dictated by the physics of the problem. The second condition, $\tilde{u}^1$, must then be such that its influence disappears in the limit $\Delta t \rightarrow 0$. This will be the case with the explicit Euler scheme $\tilde{u}^1 = \tilde{u}^0 + \Delta t Q$ [where $Q(t^0, \tilde{u}^0)$ stands for the other terms in the equation at

time t^0]. Indeed, $\tilde{u}^1$ tends to the actual initial value $\tilde{u}^0$ and the first leapfrog step yields $\tilde{u}^2 = \tilde{u}^0 + 2\Delta t Q(t^1, \tilde{u}^0 + \mathcal{O}(\Delta t))$, which is consistent with a finite difference over a $2\Delta t$ time step.

Leaving for later sections the complexity of the additional conditions that may be required by virtue of the discretization schemes, the following sections present the boundary conditions that are most commonly encountered in GFD problems. They stem from basic physical requirements.

4.6.1 Kinematic Conditions

A most important condition, independent of any physical property or subgrid-scale parameterization, is that air and water flows do not penetrate land.[5] To translate this impermeability requirement into a mathematical boundary condition, we simply express that the velocity must be tangent to the land boundary, that is, the gradient vector of the boundary surface and the velocity vector are orthogonal to each other.

Consider the solid bottom of the domain. With this boundary defined as $z - b(x, y) = 0$, the gradient vector is given by $[\partial(z-b)/\partial x,\ \partial(z-b)/\partial y,\ \partial(z-b)/\partial z] = [-\partial b/\partial x, -\partial b/\partial y, 1]$, the boundary condition is

$$w = u\frac{\partial b}{\partial x} + v\frac{\partial b}{\partial y} \quad \text{at the bottom.} \tag{4.28}$$

We can interpret this condition in terms of a fluid budget at the bottom (Fig. 4.2) or alternatively as the condition that the bottom is a material surface of the fluid, not crossed by the flow and immobile. Expressing that the bottom is a material surface indeed demands

$$\frac{\mathrm{d}}{\mathrm{d}t}(z-b) = 0, \tag{4.29}$$

which is equivalent to Eq. (4.28) since $\mathrm{d}z/\mathrm{d}t = w$ and $\partial b/\partial t = 0$.

At a *free surface*, the situation is similar to the bottom except for the fact that the boundary is moving with the fluid. If we exclude overturning waves, the position of the surface is uniquely defined at every horizontal point by its vertical position η (Fig. 4.3), and $z - \eta = 0$ is the equation of the boundary. We then express that it is a material surface[6]:

$$\frac{\mathrm{d}}{\mathrm{d}t}(z-\eta) = 0 \quad \text{at the free surface} \tag{4.30}$$

---

[5] There is no appreciable penetration of land by water and air at geophysical scales. For ground flows, known to have a strong impact on geochemical behaviors of coastal systems, an appropriate flux can always be imposed if necessary.

[6] Exceptions are evaporation and precipitation at the air–sea interface. When important, these may be accommodated in a straightforward manner.

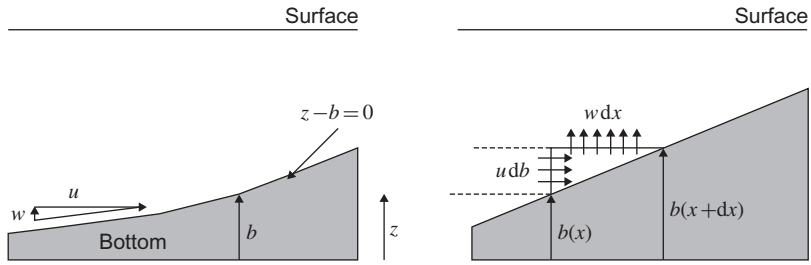

FIGURE 4.2 Notation and two physical interpretations of the bottom boundary condition illustrated here in a (x, z) plane for a topography independent of y. The impermeability of the bottom imposes that the velocity be tangent to the bottom defined by $z-b=0$. In terms of the fluid budget, which can be extended to a finite-volume approach, expressing that the horizontal inflow matches the vertical outflow requires $u\,(b(x+dx)-b(x))=w\,dx$, which for $dx\to 0$ leads to Eq. (4.28). Note that the velocity ratio w/u is equal to the topographic slope db/dx, which scales like the ratio of vertical to horizontal length scales, i.e., the aspect ratio.

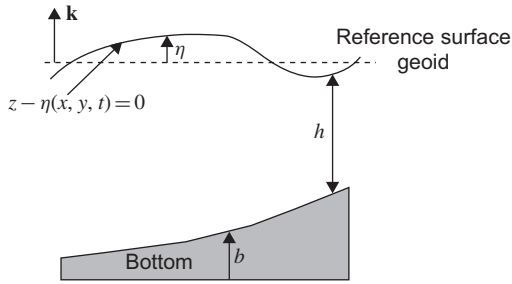

FIGURE 4.3 Notation for the surface boundary condition. Expressing impermeability of the moving surface $z=\eta$ results in boundary condition (4.31). The elevation of the sea surface height η is exaggerated compared to h for the purpose of illustration.

and obtain the surface boundary condition

$$w=\frac{\partial\eta}{\partial t}+u\frac{\partial\eta}{\partial x}+v\frac{\partial\eta}{\partial y}\quad\text{at}\quad z=\eta. \tag{4.31}$$

Particularly simple cases are those of a flat bottom and of a free surface of which the vertical displacements are neglected (such as small water waves on the surface of the deep sea)—called the *rigid-lid* approximation, which will be scrutinized in Section 7.6. In such cases, the vertical velocity is simply zero at the corresponding boundary.

A difficulty with the free surface boundary arises because the boundary condition is imposed at $z=\eta$, that is, at a location changing over time, depending on the flow itself. Such a problem is called a *moving boundary problem*, a topic which is a discipline unto itself in computational fluid dynamics (CFD) (e.g., Crank, 1987).

In oceanic models, lateral walls are introduced in addition to bottom and top boundaries so that the water depth remains nonzero all the way to the edge (Fig. 4.4). This is because watering and dewatering of land that would otherwise

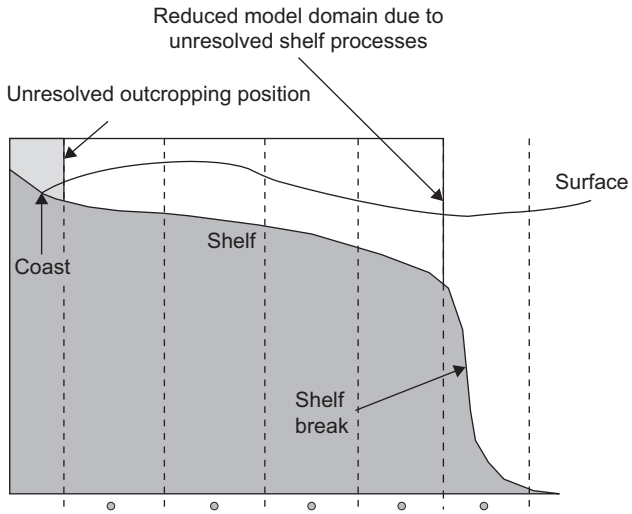

FIGURE 4.4 Vertical section across an oceanic domain reaching the coast. Besides surface and bottom boundaries, the coast introduces an additional *lateral* boundary. Introducing an artificial vertical wall is necessary because a fixed numerical grid cannot describe well the exact position of the water's edge. Occasionally, a vertical wall is assumed at the shelf break, removing the entire shelf area from the domain, because the reduced physics of the model are incapable of representing some processes on the shelf.

occur at the outcrop of the ocean floor is difficult to model with a fixed grid. At a vertical wall, impermeability demands that the normal component of the horizontal velocity be zero.

4.6.2 Dynamic Conditions

The previous impermeability conditions are purely kinematic, involving only velocity components. Dynamical conditions, implicating forces, are sometimes also necessary, for example, when requiring continuity of pressure at the air–sea interface.

Ignoring the effect of surface tension, which is important only for very short water waves (*capillary* waves, with wavelengths no longer than a few centimeters), the pressure p_{atm} exerted by the atmosphere on the sea must equal the total pressure p_{sea} exerted by the ocean onto the atmosphere:

$$p_{\text{atm}} = p_{\text{sea}} \quad \text{at air–sea interface.} \tag{4.32}$$

If the sea surface elevation is η and pressure is hydrostatic below, it follows that continuity of pressure at the actual surface $z = \eta$ implies

$$p_{\text{sea}}(z = 0) = p_{\text{atm at sea level}} + \rho_0 g \eta \tag{4.33}$$

at the more convenient reference sea level $z = 0$.

Another dynamical boundary condition depends on whether the fluid is considered inviscid or viscous. In reality, all fluids are subject to internal friction so that, in principle, a fluid particle next to fixed boundary must adhere to that boundary and its velocity be zero. However, the distance over which the velocity falls to zero near a boundary is usually short because viscosity is weak. This short distance restricts the influence of friction to a narrow band of fluid along the boundary, called a *boundary layer*. If the extent of this boundary layer is negligible compared to the length scale of interest, and generally it is, it is permissible to neglect friction altogether in the momentum equations. In this case, slip between the fluid and the boundary must be allowed, and the only boundary condition to be applied is the impermeability condition.

However, if viscosity is taken into account, zero velocity must be imposed at a fixed boundary, whereas along a moving boundary between two fluids, continuity of both velocity and tangential stress is required. From the oceanic point of view, this requires

$$\rho_0 \nu_{\mathrm{E}} \left(\frac{\partial u}{\partial z} \right) \Bigg|_{\text{at surface}} = \tau^x, \quad \rho_0 \nu_{\mathrm{E}} \left(\frac{\partial v}{\partial z} \right) \Bigg|_{\text{at surface}} = \tau^y \tag{4.34}$$

where τ^x and τ^y are the components of the wind stress exerted by the atmosphere onto the sea. These are usually taken as quadratic functions of the wind velocity $\mathbf{u}_{10}$ 10 meters above the sea and parameterized using a drag coefficient:

$$\tau^x = C_{\mathrm{d}}\, \rho_{\mathrm{air}}\, U_{10} u_{10}, \quad \tau^y = C_{\mathrm{d}}\, \rho_{\mathrm{air}}\, U_{10} v_{10}, \tag{4.35}$$

where u_{10} and v_{10} are the x and y components of the wind vector $\mathbf{u}_{10}$, $U_{10} = \sqrt{u_{10}^2 + v_{10}^2}$ is the wind speed, and C_{d} is a drag coefficient with approximate value of 0.0015 for wind over the sea.

Finally, an edge of the model may be an *open boundary*, by which we mean that the model domain is terminated at some location that cuts across a broader natural domain. Such a situation arises because computer resources or data availability restrict the attention to a portion of a broader system. Examples are regional meteorological models and coastal ocean models (Fig. 4.5). Ideally, the influence of the outside system onto the system of interest should be specified along the open boundary, but this is most often impossible in practice, for the obvious reason that the unmodeled part of the system is not known. However, certain conditions can be applied. For example, waves may be allowed to exit but not enter through the open boundary, or flow properties may be specified where the flow enters the domain but not where it leaves the domain. In oceanic tidal models, the sea surface may be imposed as a periodic function of time.

With increased computer power over the last decade, it has become common nowadays to *nest* models into one another, that is, the regionally limited model of interest is embedded in another model of lower spatial resolution but larger size, which itself may be embedded in a yet larger model of yet lower resolution, all the way to a model that has no open boundary (entire ocean basin or globe for the atmosphere). A good example is regional weather forecasting over a

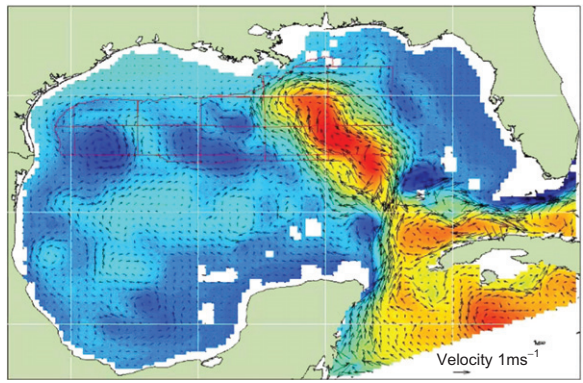

FIGURE 4.5 Open boundaries are common in regional modeling. Conditions at open boundaries are generally difficult to impose. In particular, the nature of the condition depends on whether the flow enters the domain (carrying unknown information from the exterior) or leaves it (exporting known information). (*Courtesy of the HYCOM Consortium on Data-Assimilative Modeling*). A color version can be found online at http://booksite.academicpress.com/9780120887590/

particular country: A grid covering this country and a few surrounding areas is nested into a grid that covers the continent, which itself is nested inside a grid that covers the entire globe.

4.6.3 Heat, Salt, and Tracer Boundary Conditions

For equations similar to those governing the evolution of temperature, salt, or density, that is, including advection and diffusion terms, we have the choice of imposing the value of the variable, its gradient, or a mixture of both. Prescribing the value of the variable (*Dirichlet condition*) is natural in situations where it is known from observations (sea surface temperature from satellite data, for example). Setting the gradient (*Neumann condition*) is done to impose the diffusive flux of a quantity (e.g., heat flux) and is therefore often associated with the prescription of turbulent air–sea exchanges. A mixed condition (*Cauchy condition*, *Robin condition*) is typically used to prescribe a total, advective plus diffusive, flux. For a 1D heat flux, for example, one sets the value of $uT - \kappa_T \partial T/\partial x$ at the boundary. For an insulating boundary, this flux is simply zero.

To choose the value of the variable or its gradient at the boundary, either observations are invoked or exchange laws prescribed. The most complex exchange laws are those for the air–sea interface, which involve calculation of fluxes depending on the sea surface water temperature T_{sea} (often called SST), air temperature T_{air}, wind speed $\mathbf{u}_{10}$ at 10 m above the sea, cloudiness, moisture, etc, Formally,

$$-\kappa_T \left.\frac{\partial T}{\partial z}\right|_{z=\eta} = F(T_{\text{sea}}, T_{\text{air}}, \mathbf{u}_{10}, \text{cloudiness}, \text{moisture}, \ldots). \tag{4.36}$$

For heat fluxes, imposing the condition at $z=0$ rather than at the actual position $z=\eta$ of the sea surface introduces an error much below the error in the heat flux estimate itself and is a welcomed simplification.

If the density equation is used as a combination of both salinity and temperature equations by invoking the linearized state equation, $\rho=-\alpha T+\beta S$, and if it can be reasonably assumed that all are dispersed with the same turbulent diffusivity, the boundary condition on density can be formulated as a weighted sum of prescribed temperature and salt fluxes:

$$\kappa_{\mathrm{E}}\frac{\partial\rho}{\partial z}=-\alpha\kappa_{\mathrm{E}}\frac{\partial T}{\partial z}+\beta\kappa_{\mathrm{E}}\frac{\partial S}{\partial z}. \tag{4.37}$$

For any tracer (a quantity advected and dispersed by the flow), a condition similar to those on temperature and salinity can be imposed, and in particular, a zero total flux is common when there is no tracer input at the boundary.

4.7 NUMERICAL IMPLEMENTATION OF BOUNDARY CONDITIONS

Once mathematical boundary conditions are specified and values assigned at the boundaries, we can tackle the task of implementing the boundary condition numerically. We illustrate the process again with temperature as an example.

In addition to nodes forming the grid covering the domain being modeled, other nodes may be placed exactly at or slightly beyond the boundaries (Fig. 4.6). These additional nodes are introduced to facilitate the implementation of the boundary condition. If the condition is to specify the value T_b of the numerical variable $\tilde{T}$, it is most natural to place a node at the boundary (Fig. 4.6 right side) so that

$$\tilde{T}_m=T_b \tag{4.38}$$

requires no interpolation and forms an exact implementation.

If the boundary condition is in the form of a flux, it is more practical to have two grid nodes straddling the boundary, with one slightly outside the domain and the other slightly inside (Fig. 4.6 left side). In this manner, the derivative of the variable is more precisely formulated at the location of the boundary. With the index notation of Fig. 4.6,

$$\frac{\tilde{T}_2-\tilde{T}_1}{\Delta x}\simeq\left.\frac{\partial T}{\partial x}\right|_{x_b}+\frac{\Delta x^2}{24}\left.\frac{\partial^3 T}{\partial x^3}\right|_{x_b} \tag{4.39}$$

yields a second-order approximation, and the flux boundary condition $-\kappa_T(\partial T/\partial x)=q_b$ turns into

$$\tilde{T}_1=\tilde{T}_2+\Delta x\frac{q_b}{\kappa_T}. \tag{4.40}$$

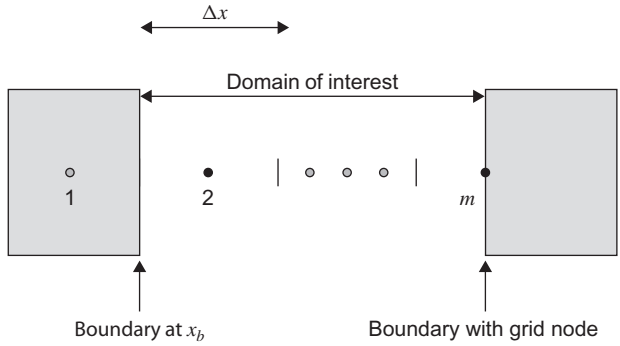

FIGURE 4.6 Grid nodes cover the interior of the domain of interest. Additional nodes may be placed *beyond* a boundary as illustrated on the left side or placed *on* the boundary as illustrated on the right. The numerical implementation of the boundary condition depends on the arrangement selected.

However, there are cases when the situation is less ideal. This occurs when a total, advective plus diffusive, flux boundary condition is specified ($uT - \kappa_T(\partial T/\partial x) = q_b$). Either the ending node is *at* the boundary, complicating the discretization of the derivative, or it is placed *beyond* the boundary, and the value of T must be extrapolated. In the latter case, extrapolation is performed with second-order accuracy,

$$\frac{\tilde{T}_1 + \tilde{T}_2}{2} \simeq T(x_b) + \frac{\Delta x^2}{8} \left.\frac{\partial^2 T}{\partial x^2}\right|_{x_b}, \tag{4.41}$$

and the total flux condition becomes

$$u_b \frac{\tilde{T}_1 + \tilde{T}_2}{2} - \kappa_T \frac{\tilde{T}_2 - \tilde{T}_1}{\Delta x} = q_b \tag{4.42}$$

yielding the following condition on the end value $\tilde{T}_1$:

$$\tilde{T}_1 = \frac{2q_b\Delta x + (2\kappa_T - u_b\Delta x)\tilde{T}_2}{2\kappa_T + u_b\Delta x}. \tag{4.43}$$

In the former case, when the ending grid node lies exactly at the boundary, the straightfoward difference

$$\frac{\partial T}{\partial x} \simeq \frac{\tilde{T}_m - \tilde{T}_{m-1}}{\Delta x} \tag{4.44}$$

provides only first-order accuracy at point x_m, and to recover second-order accuracy with this node placement, we need a numerical stencil that extends further into the domain (see Numerical Exercise 4.8). Therefore, to implement a flux

condition, the preferred placement of the ending node is half a grid step beyond the boundary. With this configuration, the accuracy is greater than with the ending point placed at the boundary itself. The same conclusion is reached for the finite-volume approach, since imposing a flux condition consists of replacing the flux calculation at the boundary by the imposed value. We immediately realize that in this case, the natural placement of the boundary is at the interface between grid points because it is the location where fluxes are calculated in the finite-volume approach.

The question that comes to mind at this point is whether or not the level of truncation error in the boundary-condition implementation is adequate. To answer the question, we have to compare this truncation error to other errors, particularly the truncation error within the domain. Since there is no advantage in having a more accurate method at the relatively few boundary points than at the many interior points, the sensible choice is to use the same truncation order at the boundary as within the domain. The model then possesses a uniform level of approximation. Sometimes, however, a lower order near the boundary may be tolerated because there are many fewer boundary points than interior points, and a locally higher error level should not penalize the overall accuracy of the solution. In the limit of $\Delta x \to 0$, the ratio of boundary points to the total number of grid points tends to zero, and the effect of less-accurate approximations at the boundaries disappears.

In Eq. (4.43), we used the boundary condition to calculate a value at a point outside of the domain so that when applying the numerical scheme at the first interior point, the boundary condition is automatically satisfied. The same approach can also be used to implement the artificial boundary conditions that are sometimes required by the numerical scheme. Consider, for example, the fourth-order discretization (1.26) now applied to spatial derivatives in the domain interior coupled with the need to impose a single boundary condition at

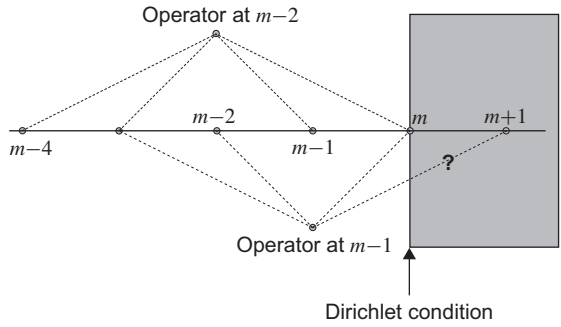

FIGURE 4.7 An operator spanning two points on each side of the calculation point can be applied only up to $m-2$ if a single Dirichlet condition is prescribed. When applying the same operator at $m-1$, we face the problem that the value at $m+1$ does not exist.

x_m of Dirichlet type. The discrete operator in the interior

$$\left.\frac{\partial T}{\partial x}\right|_{x_i} \simeq \frac{4}{3}\left(\frac{\tilde{T}_{i+1}-\tilde{T}_{i-1}}{2\Delta x}\right)-\frac{1}{3}\left(\frac{\tilde{T}_{i+2}-\tilde{T}_{i-2}}{4\Delta x}\right) \tag{4.45}$$

can be applied up to $i=m-2$. At $i=m-1$, the formula can no longer be applied, unless we provide a value at a virtual point $\tilde{T}_{m+1}$ (Fig. 4.7). This can be accomplished by requiring that a skewed fourth-order discretization near the boundary have the same effect as the centered version using the virtual value.

4.8 ACCURACY AND ERRORS

Errors in a numerical model can be of several types. Following Ferziger and Perić (1999), we classify them according to their origin.

- *Modeling errors*: This error is caused by the imperfections of the mathematical model in representing the physical system. It is thus the difference between the evolution of the real system and that of the exact solution of its mathematical representation. Earlier in this chapter, we introduced simplifications to the equations and added parameterizations of unresolved processes, which all introduce errors of representation. Furthermore, even if the model formulation had been ideal, coefficients remain imperfectly known. Uncertainties in the accompanying boundary conditions also contribute to modeling errors.
- *Discretization errors*: This error is introduced when the original equations are approximated to transform them into a computer code. It is thus the difference between the exact solution of the continuous problem and the exact numerical solution of the discretized equations. Examples are the replacement of derivatives by finite differences and the use of guesses in predictor-corrector schemes.
- *Iteration errors*: This error originates with the use of iterative methods to perform intermediate steps in the algorithm and is thus measured as the difference between the exact solution of the discrete equations and the numerical solution actually obtained. An example is the use of the so-called Jacobi method to invert a matrix at some stage of the calculations: for the sake of time, the iterative process is interrupted before full convergence is reached.
- *Rounding errors*: These errors are due to the fact that only a finite number of digits are used in the computer to represent real numbers.

A well constructed model should ensure that

$$\text{rounding errors} \ll \text{iteration errors} \ll \text{discretization errors} \ll \text{modeling errors}.$$

The order of these inequalities is easily understood: If the discretization error were larger than the modeling error, there would be no way to tell whether the mathematical model is an adequate approximation of the physical system we are

trying to describe. If the iteration error were larger than the discretization error, the claim could not be made that the algorithm generates a numerical solution that satisfies the discretized equations, etc.

In the following, we will deal neither with rounding errors (generally controlled by appropriate compiler options, loop arrangements, and double-precision instructions), nor with iteration errors (generally controlled by sensitivity analysis or a priori knowledge of acceptable error levels for the convergence of the iterations). Modeling errors are discussed when performing scale analysis and additional modeling hypotheses or simplifications (see, e.g., the Boussinesq and hydrostatic approximations) so that we may restrict our attention here to the discretization error associated with the transformation of a continuous mathematical model into a discrete numerical scheme.

The concepts of consistency, convergence, and stability mentioned in Chapter 1 only provide information on the discretization error behavior when Δt tends to zero. In practice, however, time steps (and spatial steps as well) are never tending toward zero but are kept at fixed values, and the question arises about how accurate is the numerical solution compared to the exact solution. In that case, convergence is only marginally interesting, and even inconsistent schemes, if clever, may be able to provide results that cause lower actual errors than consistent and convergent methods.

By definition, the discretization error ϵ_u on a variable u is the difference between the exact numerical solution $\tilde{u}$ of the discretized equation and the mathematical solution u of the continuous equation:

$$\epsilon_u = \tilde{u} - u. \tag{4.46}$$

4.8.1 Discretization Error Estimates

In the case of explicit discretization (2.24) of inertial oscillations, we can obtain differential equations for the errors by subtracting the modified equations (2.28) from the exact continuous equation (2.23), to the leading order:

$$\frac{\mathrm{d}\epsilon_u}{\mathrm{d}t} - f\epsilon_v = f^2 \frac{\Delta t}{2}\, \tilde{u} + \mathcal{O}(\Delta t^2)$$

$$\frac{\mathrm{d}\epsilon_v}{\mathrm{d}t} + f\epsilon_u = f^2 \frac{\Delta t}{2}\, \tilde{v} + \mathcal{O}(\Delta t^2).$$

Obviously, we are not going to solve these equations to calculate the error because it would be tantamount to solving the exact problem directly. However, what we notice is that the error equations have source terms on the order of Δt (which vanish as $\Delta t \to 0$ because the scheme is consistent) and we anticipate that these will give rise to a proportional solution for ϵ_u and ϵ_v. The truncation error of the solution should therefore be of first order:

$$\epsilon_u = \mathcal{O}(\Delta t) \sim \frac{f\Delta t}{2} \left\| \tilde{\mathbf{u}} \right\|. \tag{4.47}$$

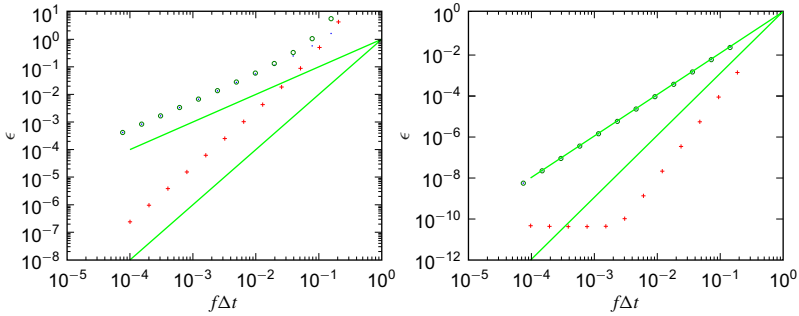

FIGURE 4.8 Relative discretization error $\epsilon = \epsilon_u / \|\tilde{u}\|$ as a function of the dimensionless variable $f\Delta t$ in the case of inertial oscillations. The log–log graphs show the real errors (dots) and estimated values of the error (circles) for an explicit scheme (left panel) and semiexplicit scheme (right panel). The slope of the theoretical convergence rates ($m = 1$ on the left panel and $m = 2$ on the right panel) are shown, as well as the next order $m+1$. Actual errors after a Richardson extrapolation (crosses) prove that the order is increased by 1 after extrapolation.

We can verify that the actual error is indeed divided by a factor 2 when the time step is halved (Fig. 4.8).

This is to be expected, since the equivalence theorem also states that for a linear problem, the numerical solution and its truncation error share the same order, say m. The difficulty with this approach is that for nonlinear problems, no guarantee can be made that this property continues to hold or that the actual error can be estimated by inspection of the modified equation.

To quantify the discretization error in nonlinear systems, we can resort to a sensitivity analysis. Suppose the leading error of the solution is

$$\epsilon_u = \tilde{u} - u = a\Delta t^m, \tag{4.48}$$

where the coefficient a is unknown and the order m may or may not be known. If m is known, the parameter a can be determined by comparing the solution $\tilde{u}_{2\Delta t}$ obtained with a double step $2\Delta t$ with the solution $\tilde{u}_{\Delta t}$ obtained with the original time step Δt:

$$\tilde{u}_{2\Delta t} - u = a2^m \Delta t^m, \quad \tilde{u}_{\Delta t} - u = a\Delta t^m \tag{4.49}$$

from which[7] falls the value of a:

$$a = \frac{\tilde{u}_{2\Delta t} - \tilde{u}_{\Delta t}}{(2^m - 1)\Delta t^m} \,. \tag{4.50}$$

[7] Notice that the difference must be done *at the same moment t*, not at the same time step *n*.

The error estimate associated with the higher resolution solution $\tilde{u}_{\Delta t}$ is

$$\epsilon_u = \tilde{u}_{\Delta t} - u = a\Delta t^m = \frac{\tilde{u}_{2\Delta t} - \tilde{u}_{\Delta t}}{(2^m - 1)}, \tag{4.51}$$

with which we can improve our solution by using Eq. (4.48)

$$\tilde{u} = \tilde{u}_{\Delta t} - \frac{\tilde{u}_{2\Delta t} - \tilde{u}_{\Delta t}}{(2^m - 1)}. \tag{4.52}$$

This suggests that the two-time-step approach may yield the exact answer because it determines the error. Unfortunately, this cannot be the case because we are working with a discrete representation of a continuous function. The paradox is resolved by realizing that, by using Eq. (4.50), we discarded higher-order terms and therefore did not calculate the exact value of a but only an estimate of it. What our manipulation accomplished was the elimination of the leading error term. This procedure is called a *Richardson extrapolation*:

$$u = \tilde{u}_{\Delta t} - \frac{\tilde{u}_{2\Delta t} - \tilde{u}_{\Delta t}}{(2^m - 1)} + \mathcal{O}\left(\Delta t^{m+1}\right). \tag{4.53}$$

Numerical calculations of the real error and error estimates according to Eq. (4.51) show good performance of the estimators in the context of inertial oscillations (Fig. 4.8). Also, the Richardson extrapolation increases the order by 1, except for the semi-implicit scheme at high resolution, when no gain is achieved because saturation occurs (Fig. 4.8, right panel). This asymptote corresponds to the inevitable rounding errors, and we can claim to have solved the discrete equations "exactly."

When considering the error estimate (4.51), we observe that the error estimate of a first-order scheme ($m = 1$) is simply the difference between two solutions obtained with different time steps. This is the basic justification for performing resolution sensitivity analysis on more complicated models: Differences in model results due to a variation in resolution may be taken as estimates of the discretization error. By extension, performing multiple simulations with different model parameter values leads to differences that are indicators of modeling errors.

When the truncation order m is not known, a third evaluation of the numerical solution, with a quadruple time step $4\Delta t$, yields an estimate of both the order m and the coefficient a of the discretization error:

$$m = \frac{1}{\log 2} \log\left(\frac{\tilde{u}_{4\Delta t} - \tilde{u}_{2\Delta t}}{\tilde{u}_{2\Delta t} - \tilde{u}_{\Delta t}}\right) \tag{4.54}$$

$$a = -\frac{\tilde{u}_{2\Delta t} - \tilde{u}_{\Delta t}}{(2^m - 1)\Delta t^m}.$$

As we can see in practice (Fig. 4.9), this estimate provides a good estimate of m when resolution is sufficiently fine. This method can thus be used to determine the truncation order of discretizations numerically, which can be useful to assess convergence rates of nonlinear discretized systems or to verify the proper numerical implementation of a discretization (for which the value of m is known). In the latter case, if a method should be of second order but the numerical estimate of m according to Eq. (4.54) reveals only first-order convergence on well behaved problems, a programming or implementation error is very likely to blame.

Having access now to an error estimate, we can think of choosing the time step so as to keep discretization errors below a prescribed level. If the time step is prescribed a priori, the error estimate allows us to verify that the solution remains within error bounds. The use of a fixed time step is common but might not be the most appropriate choice when the process exhibits a mix of slower and faster processes (Fig. 4.10). Then, it may be preferable that the time step be

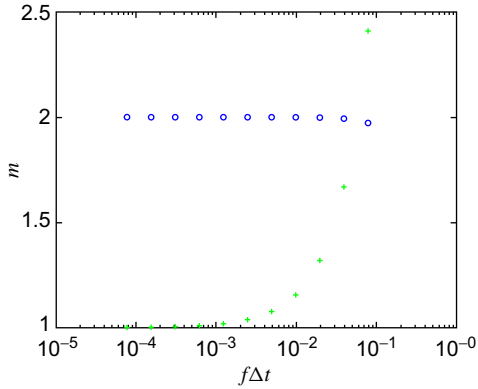

FIGURE 4.9 Estimator of m for explicit (+, tending to 1 for small time steps) and semi-implicit discretization (o, tending to 2) as function of $f\Delta t$.

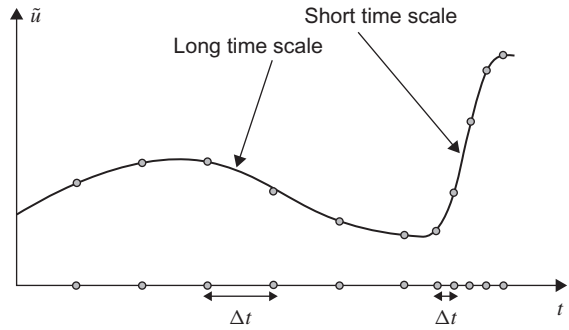

FIGURE 4.10 Use of different time steps Δt in function of the local error and time scales. The time step is decreased until the local error estimate is smaller than a prescribed value. When estimated errors are much smaller than allowed, the time step is increased.

adjusted over time so as to follow the time scale of the system. In this case, we speak about *adaptive time stepping*.

Adaptive time stepping can be implemented by decreasing the time step whenever the error estimate begins to be excessive. Vice versa, when the error estimate indicates an unnecessarily short time step, it should be allowed to increase again. Adaptive time stepping seems appealing, but the additional work required to track the error estimate (doubling/halving the time step and recomputing the solution) can exceed the gain obtained by maintaining a fixed time step, which is occasionally too short. Also, multistep methods are not easily generalized to adaptive time steps.

ANALYTICAL PROBLEMS

4.1. From the weather chart in today's edition of your newspaper, identify the horizontal extent of a major atmospheric feature and find the forecast wind speed. From these numbers, estimate the Rossby number of the weather pattern. What do you conclude about the importance of the Coriolis force? (*Hint*: When converting latitudinal and longitudinal differences in kilometers, use the Earth's mean radius, 6371 km.)

4.2. Using the scale given in Eq. (4.16), compare the dynamic pressure induced by the Gulf Stream (speed = 1 m/s, width = 40 km, and depth = 500 m) to the main hydrostatic pressure due to the weight of the same water depth. Also, convert the dynamic pressure scale in equivalent height of hydrostatic pressure (head). What can you infer about the possibility of measuring oceanic dynamic pressures by a pressure gauge?

4.3. Consider a two-dimensional periodic fluctuation of the type ($u' = U\sin(\phi+\alpha_u)$, $v' = V\sin(\phi+\alpha_v)$, $w' = 0$) with $\phi(x,y,t) = k_x x + k_y y - \omega t$ and all other quantities constant. Calculate the Reynolds stresses, such as $-\langle u'v'\rangle$, by taking the average over a 2π-period of the phase ϕ. Show that these stresses are not zero in general (proving that traveling waves may exert a finite stress and therefore accelerate or slow down a background flow on which they are superimposed). Under which relation between α_u and α_v does the shear stress $-\langle u'v'\rangle$ vanish?

4.4. Show that the horizontal eddy viscosity defined in Eq. (4.10) vanishes for a vortex flow with velocity components ($u = -\Omega y$, $v = +\Omega x$) with Ω being a constant. Is this a desirable property?

4.5. Why do we need to know the surface pressure distribution when using the hydrostatic approximation?

4.6. Theory tells us that in a pure advection problem for temperature T, a single boundary condition should be imposed at the inflow and none at the outflow, but when diffusion is present, a boundary condition must be imposed at both ends. What do you expect to happen at the outflow boundary

when diffusion is very small? How would you measure the "smallness" of diffusion?

4.7. In forming energy budgets, the momentum equations are multiplied by their respective velocity components (i.e., the $\partial u/\partial t$ equation is multiplied by u and so forth), and the results are added. Show that in this manipulation, the Coriolis terms in f and f_* cancel one another out. What would be your reaction if someone presented you with a model in which the $f_* w$ term were dropped from Eq. (4.7a) because w is small compared to u and the term $f_* u$ were retained in Eq. (4.7c) for the same reason?

NUMERICAL EXERCISES

4.1. When air and sea surface temperatures, T_{air} and T_{sea}, are close to each other, it is acceptable to use a linearized form to express the heat flux across the air–sea heat interface, such as

$$-\kappa_T \frac{\partial T_{\text{sea}}}{\partial z} = \frac{h}{\rho_0 C_v} (T_{\text{sea}} - T_{\text{air}}), \tag{4.55}$$

where h is an exchange coefficient in $(\mathrm{W\,m^{-2}\,K^{-1}})$. The coefficient multiplying the temperature difference $T_{\text{sea}} - T_{\text{air}}$ has the units of a velocity and, for this reason, is sometimes called *piston velocity* in the context of gas exchange between air and water. Implement this boundary condition for a finite-volume ocean model. How would you calculate T_{sea} involved in the flux in order to maintain second-order accuracy of the standard second derivative within the ocean domain?

4.2. In some cases, particularly analytical and theoretical studies, the unknown field can be assumed to be periodic in space. How can periodic boundary conditions be implemented in a numerical one-dimensional model, for which the discretization scheme uses one point on each side of every calculation point? How would you adapt the scheme if the interior discretization needs two points on each side instead? Can you imagine what the expression *halo* used in this context refers to?

4.3. How do you generalize periodic boundary conditions (see preceding problem) to two dimensions? Is there an efficient algorithmic scheme that ensures periodicity without particular treatment of corner points? (*Hint*: Think about a method/order of copying rows/columns that ensure proper values in corners.)

4.4. Assume you implemented a Dirichlet condition for temperature along a boundary on which a grid node exists but would like to diagnose the heat

flux across the boundary. How would you determine the turbulent flux at that point with third-order accuracy?

4.5. Models can be used on parallel machines by distributing work among different processors. One of the possibilities is the so-called *domain decomposition* in which each processor is dedicated to a portion of the total domain. The model of each subdomain can be interpreted as an open-boundary model. Assuming that the numerical scheme for a single variable uses q points on each side of the local node, how would you subdivide a one-dimensional domain into subdomains and design data exchange between these subdomains to avoid the introduction of new errors? Can you imagine the problems you are likely to encounter in two dimensions? (*Hint*: Think how periodic boundary conditions were handled in the halo approach of the preceding two problems.)

4.6. Develop a MATLAB™ program to automatically calculate finite-difference weighting coefficients a_i for an arbitrary derivative of order p using l points to the left and m points to the right of the point of interest:

$$\left.\frac{\mathrm{d}^p\tilde{u}}{\mathrm{d}t^p}\right|_{t_n} \simeq a_{-l}\tilde{u}^{n-l}+\cdots+a_{-1}\tilde{u}^{n-1}+a_0\tilde{u}^n+a_1\tilde{u}^{n+1}+\cdots+a_m\tilde{u}^{n+m}. \tag{4.56}$$

The step is taken constant. Test your program on the fourth-order approximation of the first derivative. (*Hint*: Construct the linear system to be solved by observing that Δt should cancel out in all terms except for the relevant derivative so that $\Delta t^p a_i$ can be chosen as the unknowns.)

4.7. Imagine that you perform a series of simulations of the same model with time steps of $8\Delta t$, $4\Delta t$, $2\Delta t$, and Δt. The numerical discretization scheme is of order m. Which combination of the different solutions would best approximate the exact solution, and what truncation order would the combined solution have?

4.8. For a grid node placed on the boundary, show that using the value

$$\tilde{T}_m = \frac{2}{3}\left(-\Delta x\frac{q_b}{\kappa_T}-\frac{1}{2}\tilde{T}_{m-2}+2\tilde{T}_{m-1}\right) \tag{4.57}$$

allows us to impose a flux condition at node m with second-order accuracy.

Osborne Reynolds
1842–1912

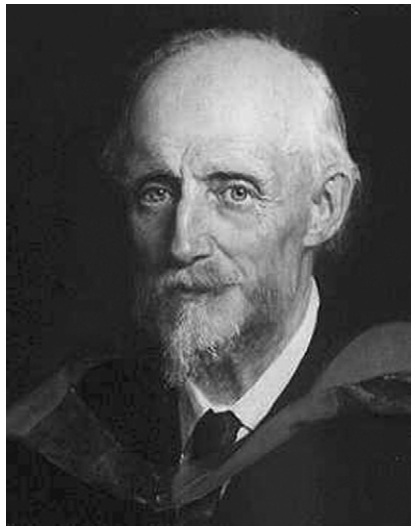

Osborne Reynolds was taught mathematics and mechanics by his father. While a teenager, he worked as an apprentice in the workshop of a mechanical engineer and inventor, where he realized that mathematics was essential for the explanation of certain mechanical phenomena. This motivated him to study mathematics at Cambridge, where he brilliantly graduated in 1867. Later, as a professor of engineering at the University of Manchester, his teaching philosophy was to subject engineering to mathematical description while also stressing the contribution of engineering to human welfare. His best known work is that on fluid turbulence, famous for the idea of separating flow fluctuations from the mean velocity and for his study of the transition from laminar to turbulent flow, leading to the dimensionless ratio that now bears his name. He made other significant contributions to lubrication, friction, heat transfer, and hydraulic modeling. Books on fluid mechanics are peppered with the expressions Reynolds number, Reynolds equations, Reynolds stress, and Reynolds analogy. (*Photo courtesy of Manchester School of Engineering*)

Carl-Gustaf Arvid Rossby
1898–1957

A Swedish meteorologist, Carl-Gustav Rossby is credited with most of the fundamental principles on which geophysical fluid dynamics rests. Among other contributions, he left us the concepts of radius of deformation (Section 9.2), planetary waves (Section 9.4), and geostrophic adjustment (Section 15.2). However, the dimensionless number that bears his name was first introduced by the Soviet scientist I. A. Kibel' in 1940.

Inspiring to young scientists, whose company he constantly sought, Rossby viewed scientific research as an adventure and a challenge. His accomplishments are marked by a broad scope and what he liked to call the *heuristic approach*, that is, the search for a useful answer without unnecessary complications. During a number of years spent in the United States, he established the meteorology departments at MIT and the University of Chicago. He later returned to his native Sweden to become the director of the Institute of Meteorology in Stockholm. (*Photo courtesy of Harriet Woodcock*)